Aerodynamic Study of Air Flow over A Curved Fin Rocket

Open Access

Md Nizam Dahalan[1,*], Ahmad Fitri Suni[1], Iskandar Shah Ishak[1], Nik Ahmad Ridhwan Nik Mohd[1], Shabudin Mat[1]

[1] Department of Aeronautical, Automotive and Ocean Engineering, Faculty of Mechanical Engineering, Universiti Teknologi Malaysia, 81310 Skudai, Johor, Malaysia

ARTICLE INFO	ABSTRACT
	This paper summarizes a study of the aerodynamic characteristics of a curved fin rocket. The study was conducted with the use of semi-empirical method and numerical simulation. The semi-empirical method was implemented with USAF DATCOM as a reference. The ANSYS Fluent was used for the numerical simulation. The curved fin rocket configuration included a conical nose, a cylindrical body, and four curved fins attached symmetrically at the aft body of the rocket. The semi-empirical method and numerical simulations were undertaken at various Mach numbers, which were 0.15, 0.4, 0.6 and 0.8 for subsonic speed. For supersonic speed, the Mach numbers were 1.2, 1.4 and 2.0. The angle of attack varied from 0˚ to 25˚ for each speed, at 5˚ increments. The compared results included those attained from wind tunnel testing, USAF DATCOM, numerical simulation, and those results gathered from previous researchers. According to the results, each method resulted in the same trend, and followed typical rocket aerodynamic characteristic trends.

1. Introduction

The rocket is one of the greatest inventions developed by human beings. The first rocket was created in China in 1200, and its first use was as fireworks during Chinese New Year celebrations [1].

Currently rockets are being utilised in various fields, including in space exploration, and by military force. Their role in space exploration can be observed clearly when modern nations such as Russia, the US, India, France and China, use rockets as the basis of their spacecraft. Rockets are used to transport humans to outer space, possessing sufficient thrust to overcome the earth's gravitational force. The Soyuz and Saturn rockets are prominent examples. Rockets act as the preliminary booster for transporting the space shuttle, and satellites, into outer space.

---

* Corresponding author.
E-mail address: nizamdahalan@utm.my (Md Nizam Dahalan)

Additionally, rockets with curved fins have been broadly used for military purposes. Within the military field, curved fin rockets are very beneficial because they can be stored in a minimal space. This can be done by keeping the fins surrounding the rocket body retracted, while it lies in the tube launcher. With the necessary storage area reduced in size, an aircraft or a rocket launcher can accommodate more rockets. With this advantage, labour can be saved in reloading processes, or in carrying extra rockets to the battlefield.

Studies of the aerodynamic characteristics of straight and curved fin rockets, and of air flow over their fins, have been undertaken by many previous researchers including Yao [2], Sethunathan *et al*. [3], Eastmen and Wenndt [4], Mandić [5], Cent [6] and Dahalan *et al*. [7]. The approaches they used included wind tunnel testing, the computational fluid dynamic (CFD) approach, and analytical analysis. Each of method has its own advantages and disadvantages, while the best approach to the study has been considered to be the use of wind tunnel testing and flight tests [8-12]. However, these methods are expensive and time-consuming. Therefore, most researchers make use of analytical analysis tools, such as the US Air Force Missile DATCOM (97 Version), the USAF Stability and Control DATCOM, and the Naval Surface Warfare Centre Dahlgren Division AP98 [13]. In regards to computational analysis, relevant tools include ANSYS (Fluent), Naviar-Stokes Code, iSight, and Cyber 175 [2, 14]. Accordingly, in this study, USAF, DATCOM, and CFD approach were all used to calculate lift, drag, and pitching moment coefficient. The air flow pattern around the rocket was also studied, using the computational fluid dynamic approach [15]. The results obtained were then compared with wind tunnel testing data.

2. Curved Fin Rocket Specifications and Configurations

The design of the curved fin rocket is shown in Figs. 1 and 2. The specifications and configurations of the rocket are shown in Table 1 and Table 2. As can be seen from the table, the rocket configuration consisted of a conical nose, a cylinder body, and four curved fins [2, 16].
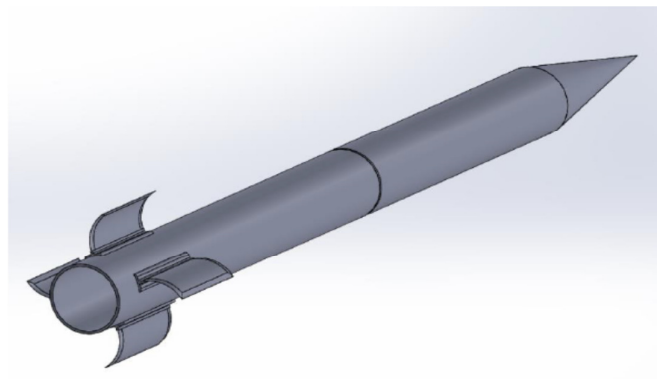
Fig. 1**.** Isometric 3D View of the Curved Fin Rocket
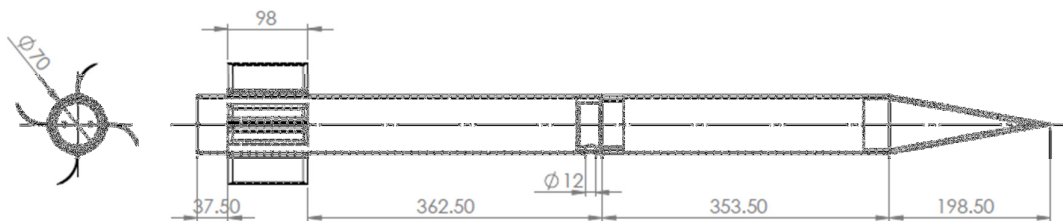
Fig. 2. Dimensions of the Curved Fin Rocket

Penerbit
Akademia Baru

Table 1
General Description of the Curved Fin Rocket

Rocket Model (body)	UTM-X1
Overall Length, L	1050 mm
Body Diameter, D	70 mm
Nose Type, Length, l_N	Conical, 198.5 mm
Afterbody Length, l_A	851.5 mm
L/D ratio	15
Weight Without Warhead	2.4529 kg
Warhead	WDU-500X/B GPF
Boat-tail	Nil

Table 2
Curved Fin Description

Fin Planform	Rectangular
Fin Configuration	Curved fin
Fin Cross Section	Double Wedge
Spanwise length of one fin, b	67.89 mm
Root Chord, cr	98 mm
Fin Thickness, t	2 mm
Fin Taper Ratio, λ	1
Fin Leading Edge Sweptback Angle, ΛL	0°

3. USAF DATCOM Method

USAF DATCOM is an analytical analysis, which uses a semi-empirical method approach [17]. The specifications and configurations of the curved fin rocket were determined for the purpose of calculations. This analysis was broken down into three parts, including those focusing on the fin alone, on the body alone, and on the fin-body combination. The speed regimes included subsonic and supersonic speeds. For subsonic speed the Mach numbers were 0.15, 0.4, 0.6 and 0.8. For Supersonic speed, the Mach numbers were 1.2, 1.4 and 2.0. The analysis was undertaken at various angles of attack, including 0°,5°,10°,15° ,20° and 25°.

The equations used to calculate the aerodynamic characteristics of the curved fin rocket at a subsonic speed are shown below. To calculate the normal force and drag coefficients, eqns. 1 and 2 were used respectively.

$$C_N = \left\{ (CN)_N \frac{S_{Nref}}{S_e} + \left[K_{F(B)} + K_{B(F)} \right] (C_N)_e \right\} \frac{Se}{Sw} + I_{VB(F)} \left(\frac{\Gamma}{2\pi Vr} \right) \frac{r}{bw/2} \frac{q}{q_\infty} \alpha (CL_\alpha)_F \tag{1}$$

$$(C_D)_{FB} = (C_{Do})_{FB} + (C_{DL})_{FB} \tag{2}$$

where, $(CN)_N$ is the normal force coefficient for bodies, $K_{F(B)}$ and $K_{B(F)}$, represent the fin lift in presence of body and the body lift in the presence of fin respectively to the fin alone lift, $(C_N)_e$ is the exposed normal force coefficient, $I_{VB(F)}$ is the vortex interference factor, S_w is the wing area, S_{Nref} is the reference area, S_e is the exposed area, α is an angle of attack, $\Gamma/2\pi Vr$ is non-dimensional vortex strength, $r/(bw/2)$ is the ratio of the radius of the body at the midpoint of the exposed root chord of the lifting panel to the semi-span of the panel, q/q_∞ is the dynamic pressure ratio, $(CL_\alpha)_F$ is the lift curve slope of the isolated gross panel, $(C_D)_{FB}$ is the fin body drag, $(C_{Do})_{FB}$ is the fin body zero lift drag and $(C_{DL})_{FB}$ is the fin body drag due to lift.

As for the supersonic speed, the normal force and drag coefficients were calculated by using Eqns. 3 and 2 consecutively. All the equations shown were for the fin-body combination, that made up the entire rocket.

$$C_N = C_{N\alpha}\frac{sin2\alpha}{2} + C_{N\alpha\alpha}sin\alpha|sin\alpha| \qquad\qquad (3)$$

where, C_N is the normal force coefficient, $C_{N\alpha}$ is the normal force curve slope and $C_{N\alpha\alpha}$ is the nonlinear coefficient based on the normal force at the maximum lift.

3. Computational Fluid Dynamic

The Computational Fluid Dynamic (CFD) capabilities have been proven in solving engineering problems for different fields such as studying heat transfer performance [18], studying turbulent flow in pipes [19] and analysing the performance of the solar updraft tower design [20]. Therefore, in this paper, the CFD simulations were conducted in order to study the aerodynamic characteristics and airflow pattern of the curved fin rocket. In the simulations, the parameter was M = 0.15, and the various angles of attack included 0°, 5°, 10°, 15° and 20°. The air flow pattern was studied, including the velocity and pressure contours of each angle of attack.
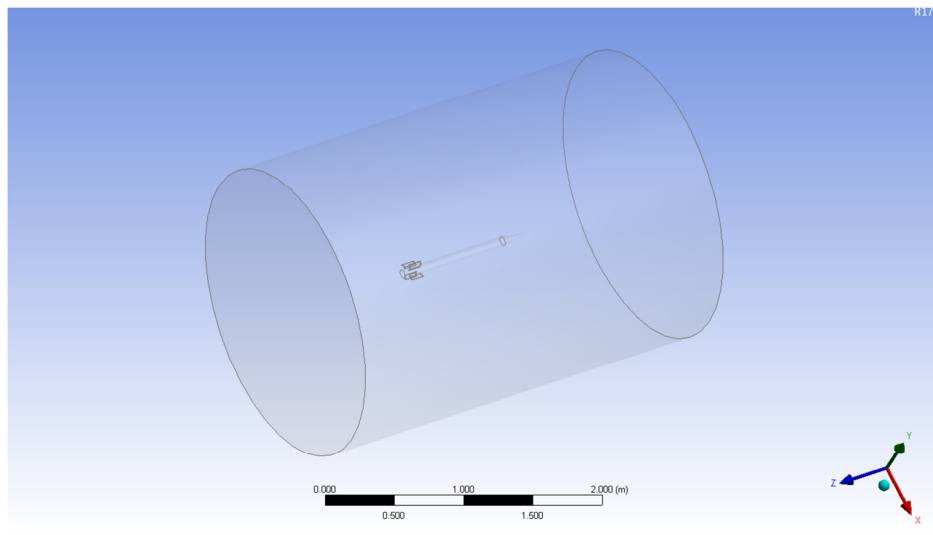

Fig. 3. Cylindrical fluid domain

In the USAF DATCOM analysis, the angles of attack have ranged up to 25°. However, in this particular analysis of CFD simulations, they only ranged up to 20°. Then, the data collection of the wind tunnel testing was chosen at M = 0.15. At this speed, Yao [2] stated that beyond 20°, the curved fin rocket started to experience vibrations. Therefore, the testing was limited to 20°.

At the workbench, important steps were undertaken involving geometry assignation, meshing generation, and setups for simulation and results. In terms of geometry, the curved fin model rocket was imported into the design modeller. At this stage, the rocket was enclosed with a cylindrical fluid domain as shown in Figure 3. The fluid domain was necessary for simulating air flow. Then the inlet, wall, rocket and outlet were assigned upon the fluid domain. The Inlet was the location from where the air flow entered, and the outlet acted as an exit from the fluid domain. The wall acted as a control volume around the rocket. The size of the fluid domain was 2m in diameter, and 3m in length.

The meshing generation of the simulation was achieved by using tetrahedron elements. This was because it was because it was easier to use, and could resolve complex geometry such as a curved fin. From Figure 4, the meshing could be considered to be denser both at the nose cone and at the curved fin. This helped ensure that the results were more accurate. The meshing near the rocket was also denser, meaning that air flow near the rocket wall could be captured. The minimum size of the meshing was 0.0001m. The smaller the element size, the higher its number. The higher the element number, the more accurate the results. However, a greater number of elements will result in a longer time required for computing results.

After the mesh generation was undertaken, the next step was to setup the simulation's boundary condition. In this setup, the *k-omega* SST viscous model was chosen. This was recommended by Li *et al*. [15] in their journal article. The SST *k-ω* turbulence model is a two-equation eddy-viscosity model. The shear stress transport (SST) formulation combines the best of the two worlds. The use of a *k-ω* formulation in the inner parts of the boundary layer made the model directly usable, all the way down to the wall, through the viscous sub-layer. Therefore, the SST *k-ω* model can be used as a Low-Reynolds turbulence model, without any extra damping functions. The SST formulation also switches to *k-ε* behaviour within a free-stream. It thereby avoids the common *k-ω* problem, wherein the model is too sensitive to inlet free-stream turbulence properties. Most authors who use the SST *k-ω* model, often merit its good behaviour to adverse pressure gradients and separating air flow. The SST *k-ω* model does produce unnecessarily large turbulence levels in regions with significant normal strain, like stagnation regions and regions with strong acceleration. This tendency is much less pronounced than in the normal k-ε model, however. Therefore, this was the model used in the study.

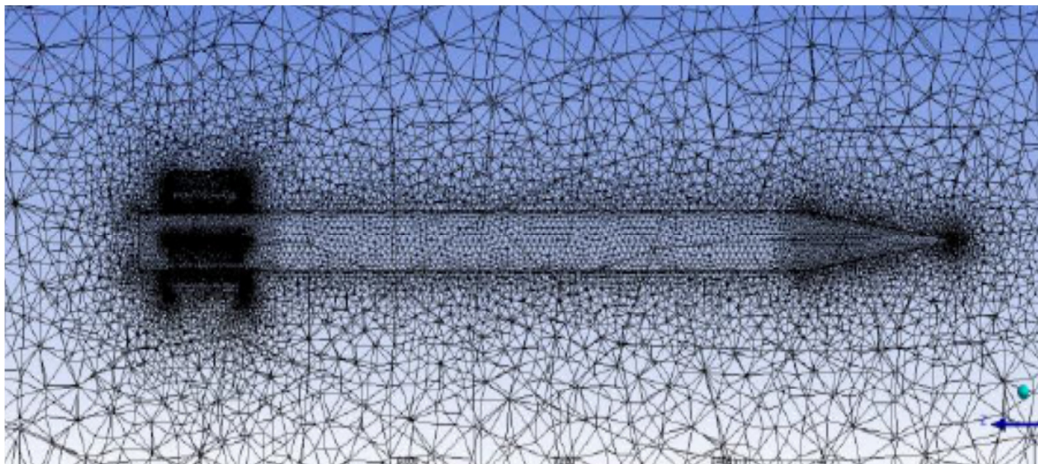**Fig. 4.** Tetrahedron Rocket Mesh

In the setup, the inlet's boundary condition was also set at various angles of attack, which were $0°, 5°, 10°, 15°$ and $20°$ at M = 0.15. The air density was 1.17 kg/m^3, which was the condition during wind tunnel testing. At the outlet, the pressure was set to zero. The wall was treated as an inlet, due to the various wind orientations. If the wall was not treated as inlet, there would be limitations due to the air flowing at the angle of attack. Therefore, with the wall as an inlet, the air flow was resolved into the y and z components in order to produce orientations. Instead of treating the wall as an inlet, the rocket body axis was changed within the fluid domain. The air flow was allowed to flow at a zero angle of attack. This gave the same results. Lastly, the simulation was run according to the assigned condition.

5. Results and Discussion

5.1 USAF DATCOM Method

5.1.1 Subsonic

Figure 5 presents the normal force coefficient, versus the angle of attack of the fin-body combination, at different Mach numbers in the subsonic regimes. It is illustrated that the normal force coefficient increased, as the angle of attack increased. The normal force coefficient at the zero angle of attack was zero. This is due to the symmetrical cylinder body, which created symmetry in terms of the rocket configuration.
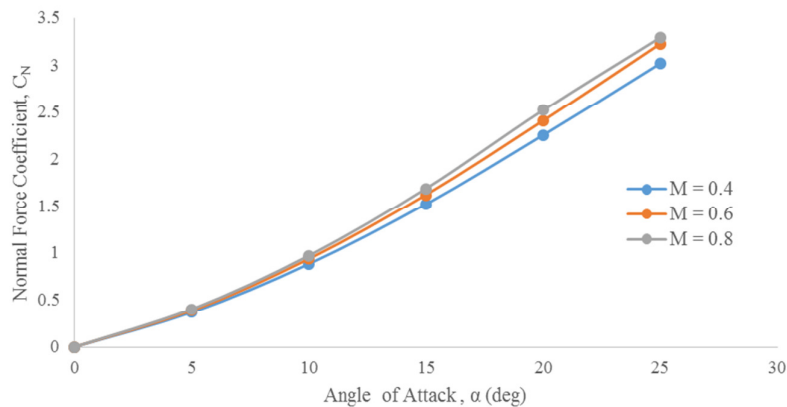
Fig. 5. Normal force coefficients at various angles of attack, at different Mach numbers, for the fin-body combination

Next, Figure 6 presents places the drag coefficient against the angle of attack of the fin-body combination, at different Mach numbers. The trend of the curve is the same with the normal force coefficient, which acts as a coefficient increase with the angle of attack. In this graph, the drag coefficient at the zero angle of attack is a positive value. This is due to the parasite drag of the rocket.
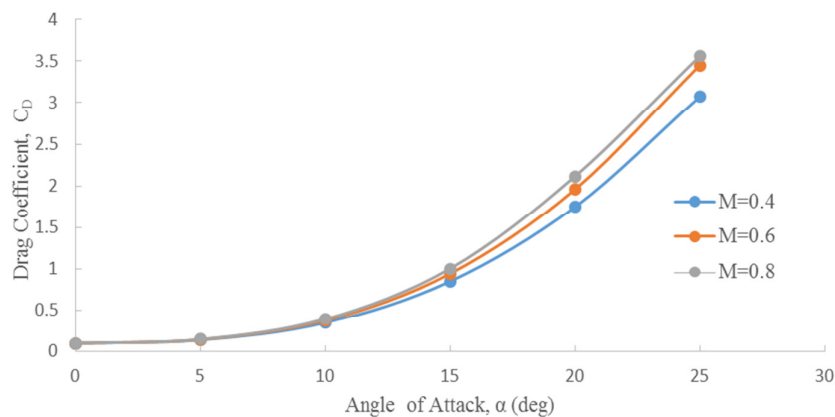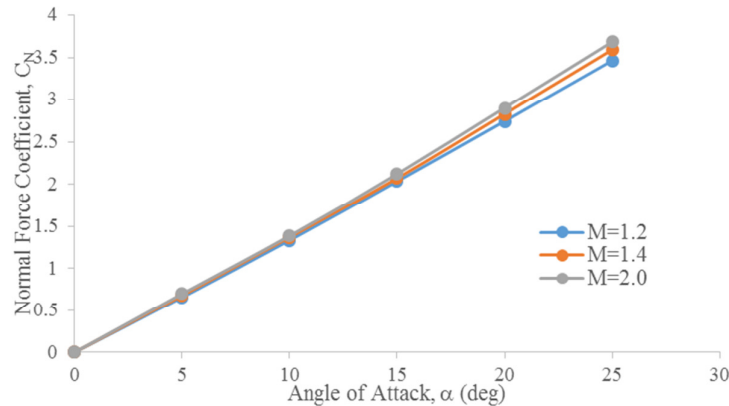

Fig. 6. Drag coefficients at various angles of attack, at different Mach numbers, for the fin-body combination

5.1.2 Supersonic

Figures 7 and 8 show the fin-body combination normal force and drag coefficients, against angles of attack at different supersonic Mach numbers. The normal force and drag coefficients increased as the angle of attack increased. The difference between the normal force coefficients of

each Mach number was little. As for the drag, the difference between each Mach number was large. The greater the Mach number, the greater the normal force and the drag coefficients.

Fig.7. Normal force coefficients at various angles of attack, at different Mach numbers, for the fin-body combination
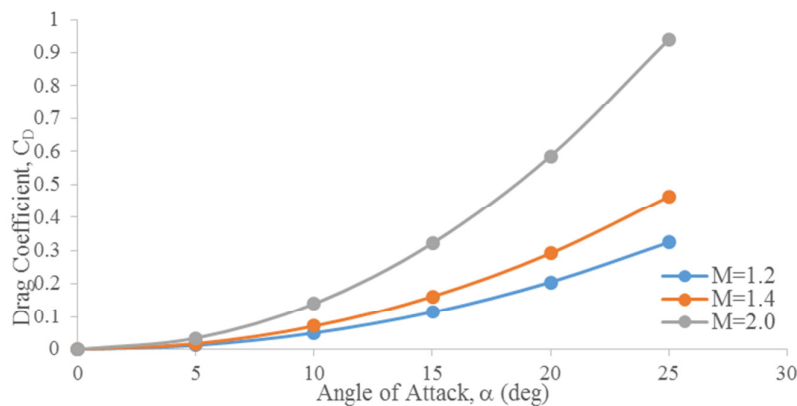
Fig. 8. Drag coefficients at various angles of attack, at different Mach numbers, for the fin-body combination

5.2 Computational Fluid Dynamics
5.2.1 Velocity and pressure contour

The following figures illustrate the velocity contours for the rocket, at each angle of attack, at M = 0.15. In Figure 9(a), at the zero angle of attack, the velocity contours at the top and bottom of the rocket showed a slow velocity profile which is at the same velocity. This is theoretically true, as the air flow around the rocket at a zero angle of attack was symmetrical. Therefore, the pressure contour in Figure 10(a) indicated that the pressure profiles at the top and bottom of the rocket appeared at the same magnitude. Therefore, there was no pressure difference on the rocket, and consequently there was zero lift at the zero angle of attack.

As the angle of attack increased, the velocity contour on the bottom of the rocket was slower than that on the top part of the rocket. This can be seen clearly in the Figure 9. This event occurred because the air flow at the top part of the rocket was faster than that at the bottom part. It was the same principle as what happened on the flat wing, where at an angle of attack the air flow was faster at the top part. Bernoulli's Principle states that the higher the velocity, the lower the pressure. At angles of attack ranging from 0°to 20°, there was a difference in pressure between the

top and the bottom of the rocket. Lift was accordingly generated. This can be observed in Figure 10.
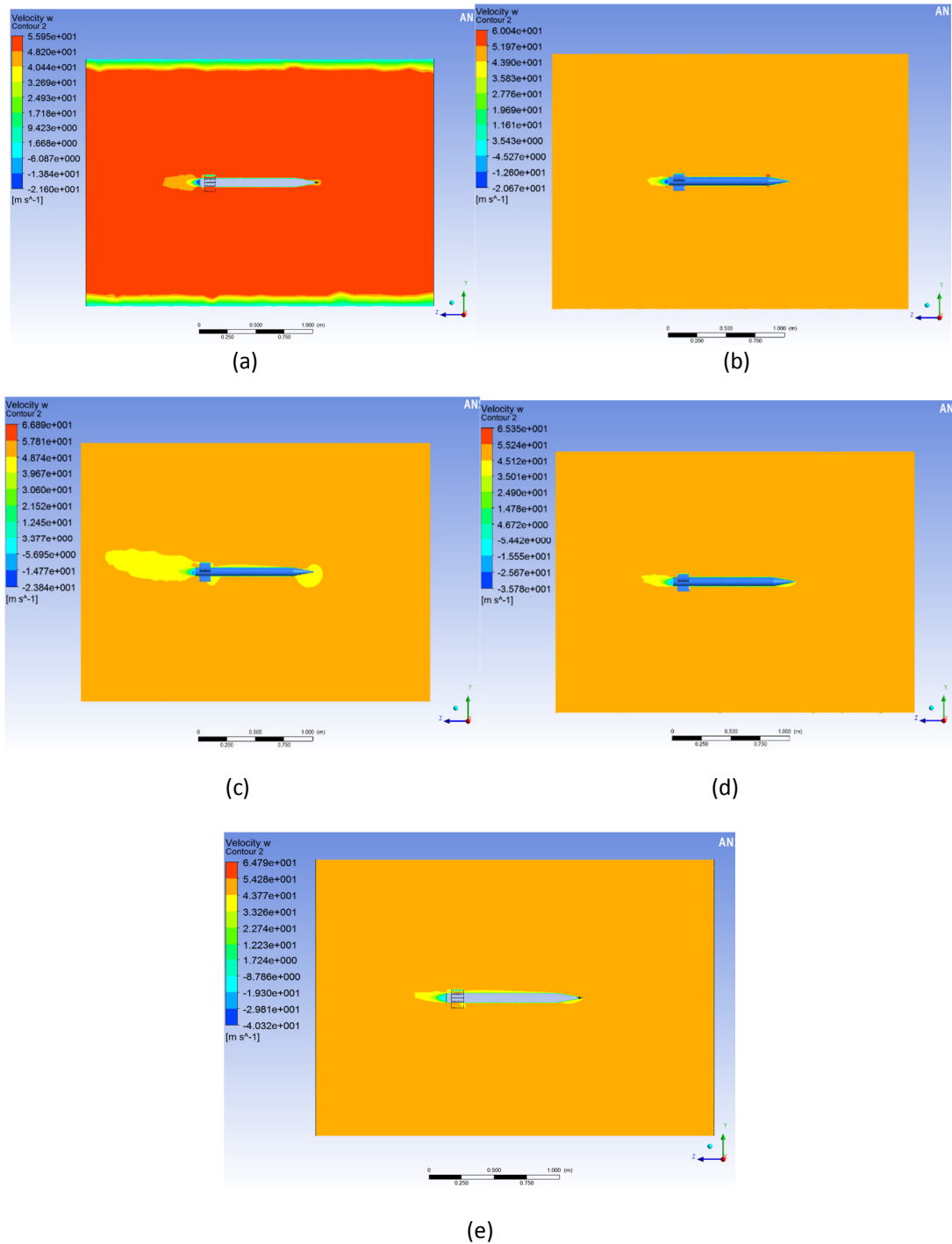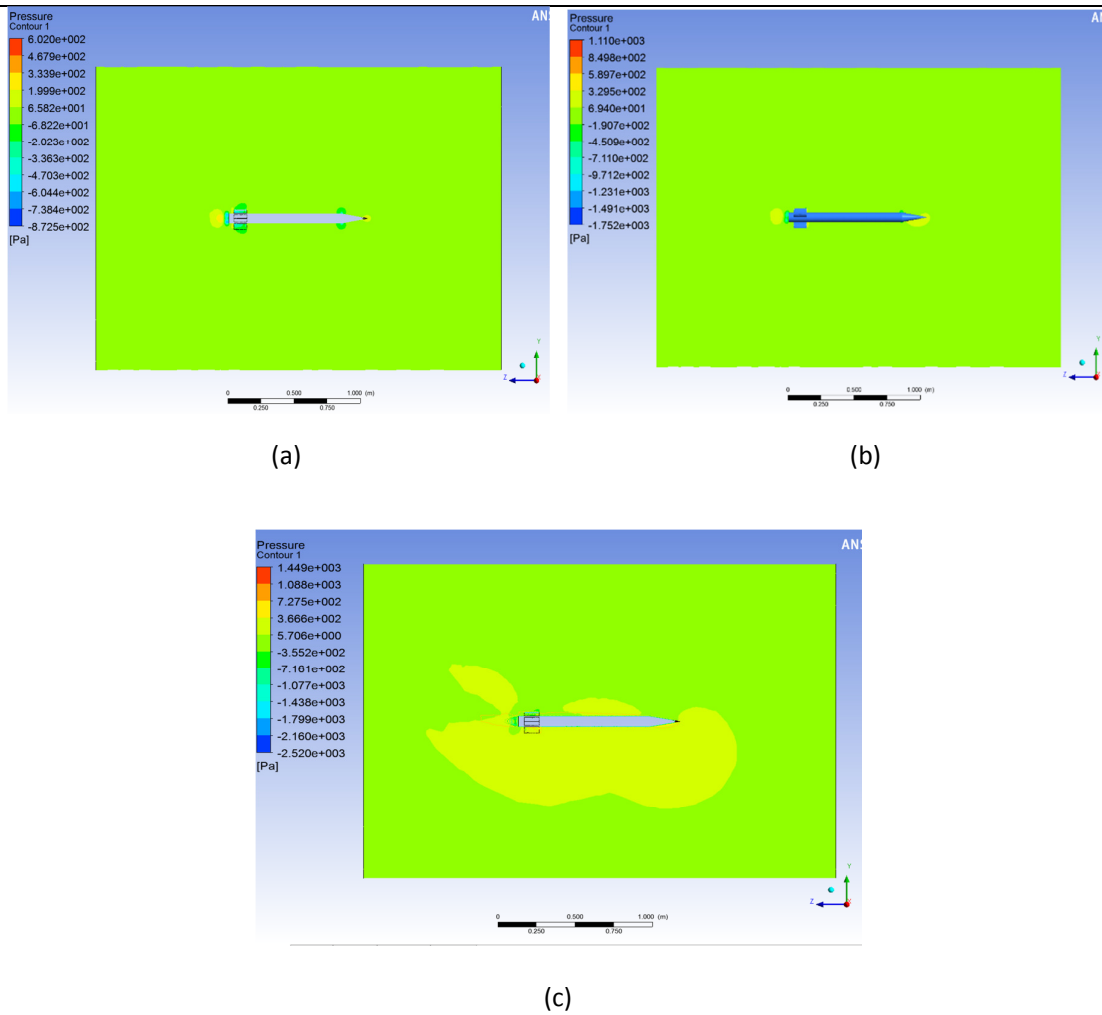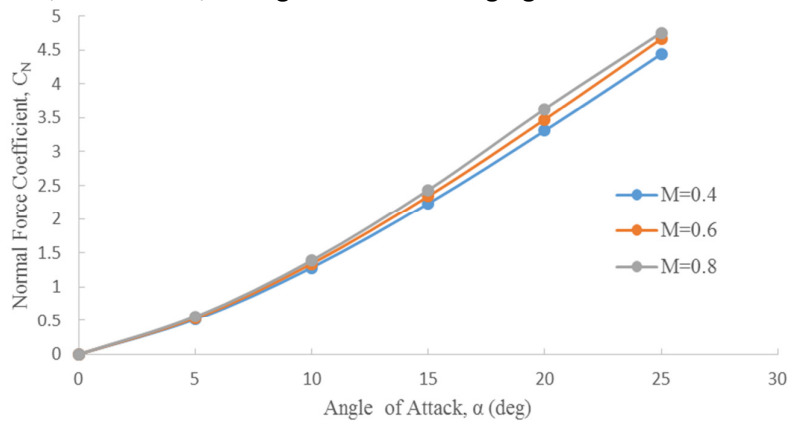

(a)

(b)

(c)

(d)

(e)

Fig. 9. Velocity contour at M=0.15 (a) α=0^0, (b) α=5^0, (c) α=10^0, (d) α=15^0, (e) α=20^0
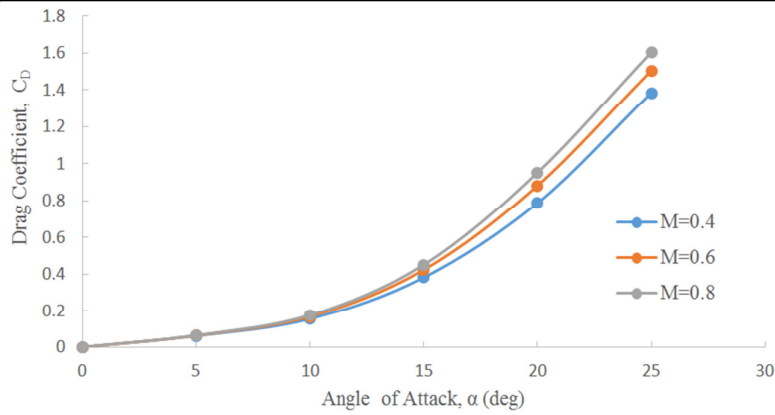
(a)

(b)

(c)

Fig. 10. Pressure Contour at M=0.15 (a) $\alpha=0^0$, (b) $\alpha=10^0$, (c) $\alpha=20^0$

5.2.2   Subsonic

Figures 11 and 12 show the results of computational fluid dynamics. The simulations were conducted at M = 0.4, 0.6 and 0.8, at angles of attack ranging from 0 to 25°.
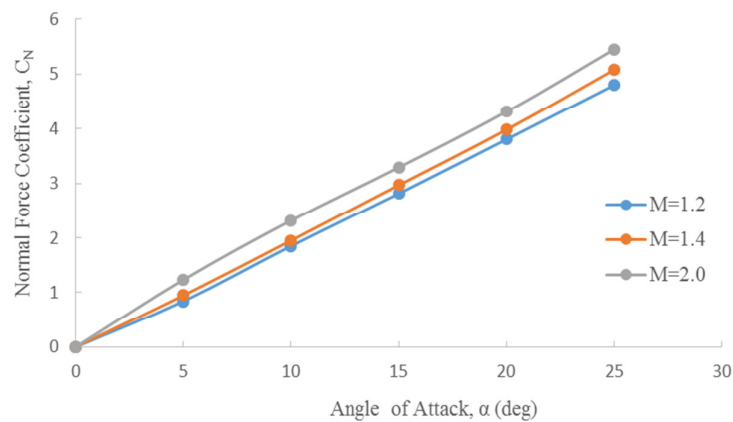

Fig. 11. Normal force coefficients at various angles of attack, for the fin-body combination, at different Mach numbers
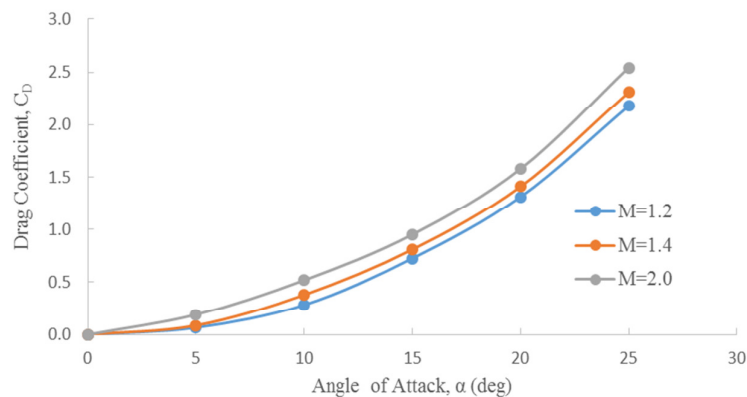
Fig. 12. Drag coefficients at various angles of attack, for the fin-body combination, at different Mach numbers

5.2.3 Supersonic

Figures 13 and 14 show the results of computational fluid dynamics. The simulations were conducted at M = 1.2, 1.4 and 2.0, at angles of attack ranging from 0 to 25˚.

Fig. 13. Normal force coefficients at various angles of attack, for the fin-body combination, at different Mach numbers

Fig. 14. Drag coefficients at various angles of attack, for the fin-body combination, at different Mach numbers

5.3 Results Comparison

Figures 15 and 16 show a data comparison between USAF DATCOM, the CFD approach, and wind tunnel testing results. Wind tunnel testing was conducted by Yao [2] at Low-Speed Tunnel, Universiti Teknologi Malaysia (UTM-LST) using the same specifications and configurations of the rocket. The data in all three graphs show the same trend. The normal force coefficients for the CFD were higher than that of the wind tunnel results. It is known that wind tunnel testing data is usually considered to be correct, as they simulate the tunnel's realistic condition. In terms of drag coefficients, the CFD data was almost the same as the wind tunnel data. The difference here was very small. Therefore, it was critical that the meshing was taken care of so that the normal force and drag coefficients would have minimal errors.
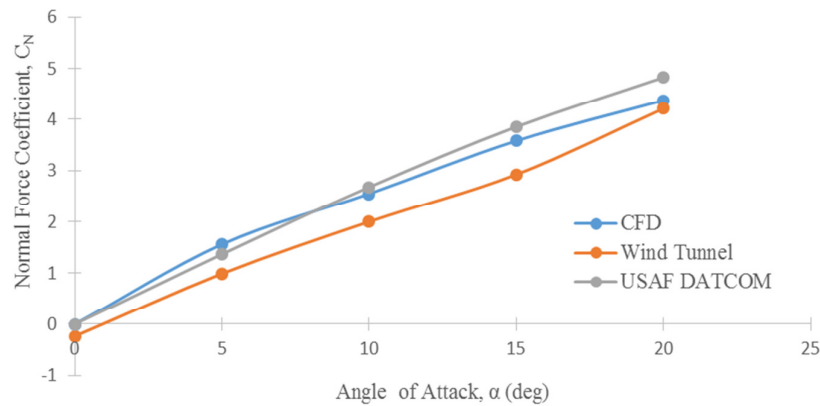

Fig. 15. Normal force coefficients at various angles of attack, at M =0
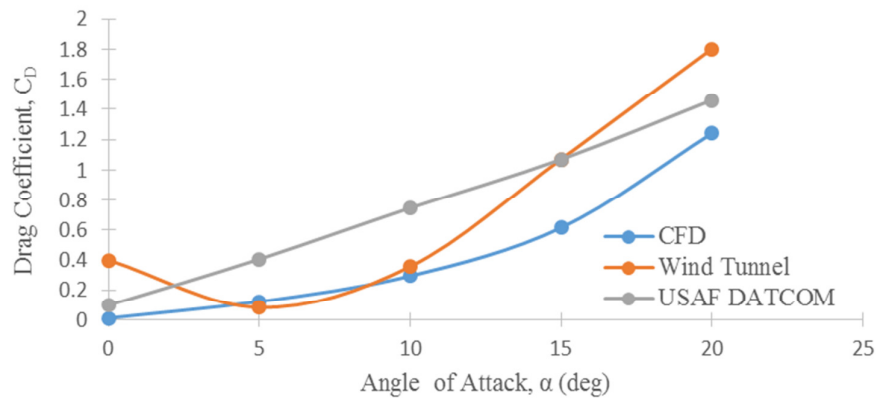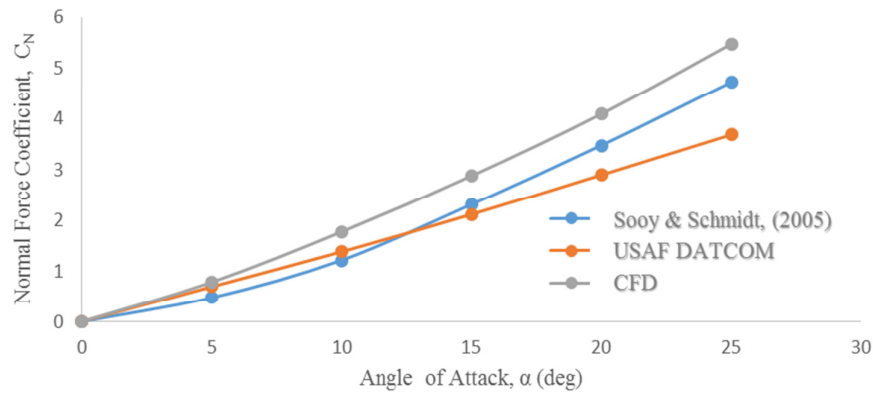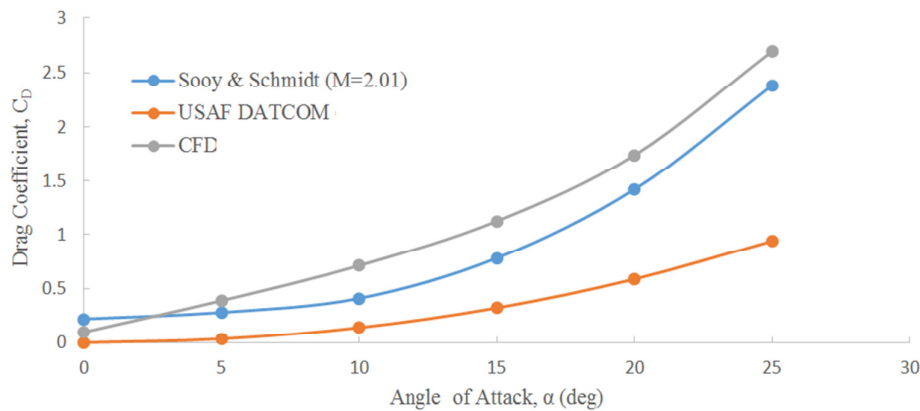

Fig. 16. Drag coefficients at various angles of attack, at M=0.15

Additionally, in terms of the USAF DATCOM analysis, the data for the normal force and drag coefficients were greater than that of both the wind tunnel and the CFD. USAF DATCOM analysis is a semi-empirical method, involving graph reading, calculation and geometry readings. As such, it was difficult to obtain the level of data precision which could be attained in a wind tunnel. However, data from the USAF DATCOM analysis was useful as a means of making preliminary predictions, and for estimating rocket aerodynamic characteristics. In terms of figures, the trend followed that of the wind tunnel and CFD. Therefore, the USAF DATCOM analysis could be used as initial guidance for the CFD simulation. Figures 17 and 18 show a comparison between the outcomes from the Sooy and Schmidt [13], USAF DATCOM and CFD at Mach number around 2.0.

Fig. 17. Normal force coefficients at various angles of attack, at M≈2.0

Fig. 18. Drag coefficients at various angles of attack, at M=0.15

6. Conclusion

In conclusion, this project was conducted in order to study air flow patterns and aerodynamic characteristics of curved fin rockets. Wind tunnel experimental data from previous researchers was used as a reference for the USAF DATCOM and the computational fluid dynamic (CFD). To study more regarding the high subsonic and supersonic speed of a curved fins rocket, USAF DATCOM was implemented as a method appropriate up to hypersonic speed. Aerodynamic characteristics can be predicted through this method. The air flow pattern around the curve fins rocket was consequently studied through the use of CFD. Through numerical simulation, this can be considered an easier and cheaper solution than wind tunnel testing. As mentioned previously, CFD is the best substitute for wind tunnels that are expensive and time-consuming. The CFD can also predict aerodynamic characteristics that include lift and drag coefficients. In this study the wind tunnel, USAF DATCOM and CFD results, all presented similar trends. It could be indicated that the CFD results of normal force and drag coefficients in agreement with the wind tunnel outcomes.

Reference

[1]   Howell, E. "Rockets : A History". Space.com Contibutor, 2015.

[2]   Yao, N. "Experimental Investigation of Curved Fin Rocket". Final Year Undergraduate Project Thesis, Universiti Teknologi Malaysia, 2015.

[3]   Sethunathan, P., R. N. Sugendran, and T. Anbarasan. "Aerodynamic Configuration Design of a Missile."

[4]   EASTMAN, D., and D. WENNDT. "Aerodynamics of maneuvering missiles with wrap-around fins." In *3rd Applied Aerodynamics Conference*, p. 4083. 1985.

[5]   Mandić, Slobodan. "Analysis of the Rolling Moment Coefficients of a Rocket With Wraparound Fins." *Serbia Military Technical Institute, Scientific Technical Review* 56, no. 2 (2006): 30-37.

[6]   Cent, Vin, and Tai Vin Cent Su. "Development of Computer Software on Rocket Aerodynamic Characteristics Estimation." PhD diss., Universiti Teknologi Malaysia, 2007.

[7]   Dahalan, Md Nizam, Su Vin Cent, and Mohd Shariff Ammoo. "Development of a computer program for rocket aerodynmic coefficients estimation." *Jurnal Mekanikal* 28 (2009): 28-43.

[8]   Seginer, A., and B. Bar-Haim. "Aerodynamics of wraparound fins." *Journal of Spacecraft and Rockets* 20, no. 4 (1983): 339-345.

[9]   Allen, Jerry M., and Carolyn B. Watson. "Experimental study at low supersonic speeds of a missile concept having opposing wraparound tails." (1994).

[10]   Pope, A. and Harper, J. "Low-speed wind tunnel testing". Technology & Engineering, 1966.

[11]   Nielsen, Jack N. "Missile aerodynamics." (1988).

[12]   Lesieutre, Daniel J., John F. Love, and Marnix FE Dillenius. "High angle of attack missile aerodynamics including rotational rates-Program M3HAX." In *Atmospheric Flight Mechanics Conference*. 1996.

[13]   Sooy, Thomas J., and Rebecca Z. Schmidt. "Aerodynamic predictions, comparisons, and validations using missile datcom (97) and aeroprediction 98 (ap98)." *Journal of spacecraft and rockets* 42, no. 2 (2005): 257-265.

[14]   Catani, U., De Amicis, R., Masullo, S., Bertin, J. and Bouslog, S. "Aerodynamic characteristics for a slender missile with wrap-around fins. Journal of Spacecraft and Rockets". 20(2), (1983): 122-128.

[15]   Li, M., Abbas, L. and Rui, X. "The Simulation of Wraparound Fins Aerodynamic Characteristics". Nanjing University of Science and Technology, 2015.

[16]   Rahman, M.R. "Wind tunnel test on UTM -X1 rocket body". Final Year Undergraduate Project Thesis, Universiti Teknologi Malaysia, 2007.

[17]   Finck, R. D., Air Force Flight Dynamics Laboratory (US), and D. E. Hoak. *USAF stability and control DATCOM*. Engineering Documents, 1978.

[18]   Qin, Yap Zi, Amer Nordin Darus, Nor Azwadi Che Sidik, and Nor Azwadi. "Numerical analysis on natural convection heat transfer of a heat sink with cylindrical pin fin." *J. Adv. Res. Fluid Mech. Therm. Sci.* 2, no. 1 (2014): 13-22.

[19]   Wong, M.K., L. C. Sheng, L.C., Che Sidik, N. A. and Hashim, G.A., "Numerical Study of Turbulent Flow in Pipe with Sudden Expansion", Journal of Advanced Research in Fluid Mechanics and Thermal Sciences, Vol. 6, No. 1, (2015): 34-48.

[20]   Too, J. H. Y., and C. S. N. Azwadi. "Numerical Analysis for Optimizing Solar Updraft Tower Design Using Computational Fluid Dynamics (CFD)." *J. Adv. Res. Fluid Mech. Therm. Sci.*22 (2016): 8-36.